EuroIntervention 2015;11:948-955 published online ahead of print August 2014

Transapical mitral valved stent implantation: computed tomographic evaluation of different prototype designs

Saskia Pokorny[1,2], MSc; Alin Heinig[1], MD; Holger Hettich[1], MD; Telse Bähr[1], DVM; Martin Marczynski-Bühlow[1], PhD; Michael M. Morlock[2], PhD; Benjamin Sattler[3], MD; Jan Schöttler[1], MD; Georg Lutter[1]*, MD, PhD

1. Department of Cardiovascular Surgery, Christian-Albrechts-University of Kiel, School of Medicine, Kiel, Germany; 2. Institute of Biomechanics, TUHH Hamburg University of Technology, Hamburg, Germany; 3. Department of Diagnostic Radiology, Christian-Albrechts-University of Kiel, School of Medicine, Kiel, Germany

KEYWORDS

- beating heart
- computed tomography
- CT comparison
- mitral valved stent
- off-pump
- transcatheter

Abstract

Aims: The evaluation of *in vivo* shaping of mitral valved stent prototypes using cardiac computed tomography (CT) was the focus of this study.

Methods and results: Twelve pigs received a self-expanding mitral valved stent, composed of an atrial element connected to a tubular ventricular body at a modified angle (45°, 90°, 110°) resulting in three designs. Cardiac CT was performed three weeks after implantation, with focus placed on stent design-related parameters: possible left ventricular outflow tract obstruction and stent shaping. CT was successfully conducted in 11/12 animals showing correct stent position within the mitral annulus and no obstruction of the left ventricular outflow tract in 9/11 animals. Minor radial deformations of the stent body were detected. At the atrioventricular junction, deformations of the stent structure were observed in all cases. Stents with a 45° angle exhibited the greatest deflection (≤56.4°±14.5°).

Conclusions: The effectiveness of cardiac computed tomography in the development process of valved stents to provide essential information and quantitative data about the *in vivo* stent geometry was demonstrated. The *in vivo* mechanical deformations of the stent were quantified, identifying critical design areas: a larger preset angle leads to less deflection and improved alignment and hence reduces the mechanical load.

**Corresponding author: Christian-Albrechts-University of Kiel, School of Medicine, Arnold Heller Str. 7, D-24105 Kiel, Germany. E-mail: georg.lutter@uksh-kiel.de*

SUBMITTED ON 20/08/2013 - REVISION RECEIVED ON 29/11/2013 - ACCEPTED ON 04/12/2013

DOI: 10.4244/EIJY14M08_14

EuroIntervention 2015;11:948-955

Introduction

The implantation of a valved stent into the mitral position in the beating heart has been the focus of recent research[1]. Such a technique would allow the treatment of elderly patients with severe comorbidities who are non-compliant to standard surgery[2]. The feasibility of transcatheter mitral valved stent implantation aiming at an off-pump replacement of the mitral valve was first reported by von Segesser and colleagues in 2005[3]. To date, promising results have been achieved in experimental development of mitral valved stents[4-6].

The *in vivo* assessment of stent design-related parameters, as well as functional parameters, is of great importance throughout the developmental process of these novel cardiac devices. Echocardiography is an established imaging method, but has reproducibility and accuracy limitations, particularly with regard to stent design-related geometric parameters[7]. Multiple studies show the benefits of cardiac computed tomography (CT) for the evaluation of different cardiac devices, such as the assessment of coronary stents or bioprosthetic aortic valve implants[8,9]. Furthermore, CT is a method increasingly utilised in the assessment and evaluation of patients undergoing transcatheter aortic valve implantation (TAVI)[10-12].

During the development process of new devices such as the mitral valved stent, cardiac CT data provide valuable information and can be used to evaluate the geometry of the valved stent in an *in vivo* setting. Apart from functional parameters, the deformation (oval deformation, angular deflection) of the valved stent *in vivo* as well as its adaptation within the native structures can be quantitatively analysed. One critical design element during stent development is the shaping of the junction between the ventricular and atrial elements. An optimal fit into the native structures has to be provided in order to reduce mechanical loading. At the same time, paravalvular sealing has to be achieved and the stent position has to be stable. In particular, a migration into the left ventricle has to be avoided. Therefore, three different stent configurations have been designed and compared. The aim of this study was the quantitative evaluation of *in vivo* shaping of these mitral valved stent prototypes by cardiac computed tomographic analysis.

Materials and methods

MITRAL VALVED STENT DESIGN

The mitral valved stent is composed of a cone-shaped atrial element connected to a tubular ventricular body. The self-expanding nitinol stent frame (Euroflex GmbH, Pforzheim, Germany) was covered with a polytetrafluoroethylene (PTFE) membrane (Zeus Inc., Orangeburg, SC, USA). A trileaflet bioprosthetic heart valve was sewn into the ventricular body and a ventricular fixation system consisting of four neochordae was attached to the ventricular rim.

The angle between atrial element and ventricular body was modified to evaluate its effect on alignment within the native anatomy of the left atrium. In this study, three different prototypes with: 1) a narrow angle of 45° (n=4), 2) a medium angle of 90° (n=4), and 3) a wide angle of 110° (n=4) were evaluated **(Figure 1)**. The nitinol stent frame of the wide-angled prototypes was manufactured from raw material with a decreased thickness.

TRANSAPICAL IMPLANTATION PROCEDURE

Twelve pigs (German Landrace and German Edelschwein) with an average body weight of 49.9±3.8 kg underwent transapical mitral valved stent implantation in an off-pump technique, as described previously[4,5]. A lower ministernotomy was performed, granting access to the apex of the heart in the porcine model[4,5,13,14]. Stent deployment and positioning was performed under transoesophageal echocardiographic (TEE) guidance (Philips iE33 xMatrix, TEE Probe X7-2t; Philips Healthcare, Best, The Netherlands). A full TEE evaluation was performed one hour after successful implantation following a comprehensive standardised protocol. All animals received humane care, as approved by the Center for Experimental Animal Research at the University of Kiel, Germany, in compliance with the "Guide for the Care and Use of Laboratory Animals" prepared by the Institute of Laboratory Animal Resources, National

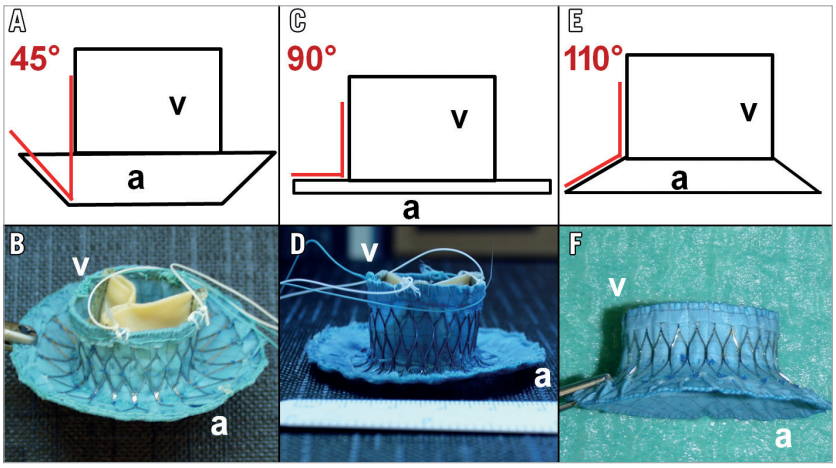

Figure 1. *Schematic drawing and image of 45° angle prototype (A & B); 90° angle prototype (C & D); and 110° angle prototype (E & F). a: atrial element; v: ventricular body*

Research Council and published by the National Academy Press, revised in 2011. Echocardiographic and haemodynamic data of pigs implanted with a mitral valved stent prototype have been published previously[4,5,13,14].

COMPUTED TOMOGRAPHY

A cardiac CT was performed three weeks after successful implantation of the mitral valved stent. The CT examination was performed under total intravenous anaesthesia and intermittent positive pressure ventilation in the supine position. To establish a baseline, a cardiac CT was performed under identical conditions prior to mitral valved stent implantation in two pigs (49.5±1.8 kg).

CT scanning was performed using a high definition 64-slice scanner (Siemens SOMATON Sensation; Siemens Healthcare, Forchheim, Germany) in the craniocaudal direction during single expiratory breath-hold and with synchronised electrocardiogram (ECG) using leads placed in the standard position.

Data were acquired with a tube voltage of 120 kV and a tube current of 770 mA. Detector collimation was 1×64×0.6 mm, slice acquisition 64×0.6 mm by means of a z-flying focal spot, tube rotation time 0.33 s, and table feed 7.68 mm per rotation. The pitch was set to 0.2. The studies were acquired after injection of 80 ml iodinated contrast media (Imeron®350; Bracco Imaging, Konstanz, Germany) followed by 60 ml of 30 percent contrast media dilution and again followed by 50 ml of saline solution. Flow rate during the injection sequence was 5 ml/s. The delay time prior to scan acquisition was estimated by injection of a 10 ml contrast medium test bolus at 5 ml/s, followed by 40 ml saline solution. The actual delay time was calculated as the time to peak contrast attenuation in the aortic bulb plus three seconds. The contrast medium was administered intravenously using a double head power injector (Injektron CT2; MedTron AG, Saarbrücken, Germany). Beta-blockers were not administered.

A retrospectively ECG-gated algorithm was used for data processing (VB40B, Syngo CT 2009E; Siemens Healthcare). The raw data were reconstructed at eleven phases of the r-r interval (0-90% at 10% intervals and at 65%) with a smooth convolution kernel (B25f) and a patient-adapted field-of-view (FOV). All images were reconstructed on a 512×512 pixel matrix at a thickness of 1 mm with 0.5 mm overlap.

DATA ANALYSIS

Analysis of the reconstructed data was performed using cardiac review software (OsiriX, v.4.1.2; Pixmeo SARL, Geneva, Switzerland) by two observers in consensus reading. The focus of this study was the evaluation of stent-design-related parameters (oval deformation, angular deflection). To quantify the expansion of the tubular stent body, minimal and maximal diameters were determined in the valvular plane and at the ventricular rim in short-axis view during mid diastole (65% ECG phase) and end systole (20% ECG phase). The contours of the stent leaflets in the valvular plane were manually drawn to calculate the effective opening area during diastole. Obstruction of the left ventricular outflow tract (LVOT) was expressed as percentage based on the opening area of the aortic valve and the LVOT during systole.

One parameter of particular interest was the deflection of the angle α between the ventricular stent body and the atrial element *in vivo*. Bearing this in mind, the parameter "angular deflection" was defined as the deviation between the angle α preset during the manufacturing process (45°, 90°, 110°) and the angle α as derived from the cardiac CT evaluation. This parameter relates directly to the mechanical forces acting upon the nitinol stent frame. To evaluate the angular deflection, the annulus was divided into four zones following Carpentier`s segmental valve analysis: anteromedial, anterolateral, posterolateral and posteromedial[15]. In each zone, the angle of the atrioventricular junction was measured in four views perpendicular to the valvular plane **(Figure 2)** during systole and diastole (20% and 65% ECG phase).

To assess possible changes of the heart geometry, the left atrial (LA) diameter, height and circumference were evaluated in four-chamber and short-axis view at maximal atrial filling and measured at a distance of 5 mm to the valvular plane. The perpendicular distance from the valvular plane to the plane between the papillary muscle heads and the apex was determined in end diastole (80%

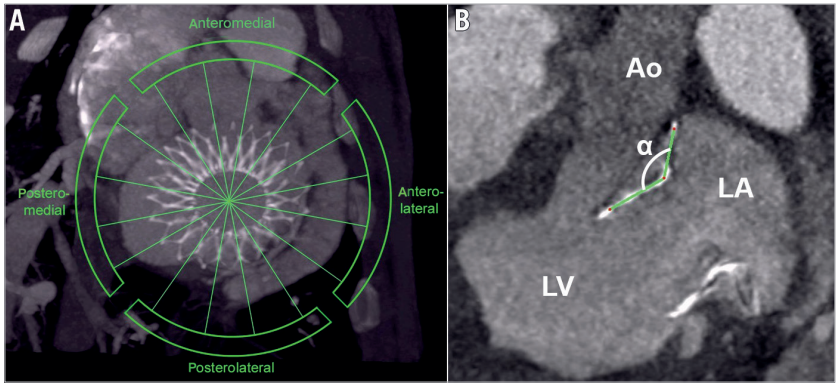

Figure 2. *Cardiac CT images acquired in mid diastole (65% ECG). A) Image showing the four zones that were defined to evaluate the angular deflection. B) View perpendicular to the valvular plane in the anteromedial zone. The nitinol stent frame was marked green. α: angle between ventricular and atrial element; Ao: aorta; LA: left atrium; LV: left ventricle*

ECG phase). Basal and mid ventricular thickness of septum and myocardium were measured in four-chamber view during end diastole. The effective valvular opening area was derived from the cardiac CT data in the valvular plane during mid diastole.

Furthermore, a volumetric left ventricular analysis was performed and the left ventricular ejection fraction (EF) was calculated. Thereafter images for end systole and end diastole were prepared as those presenting the smallest and largest luminal cavity areas, respectively, at mid ventricular level. The left ventricular endocardial contours were manually drawn into end-diastolic and end-systolic images. Papillary muscles and trabeculations were included in the volumetric analysis. A macroscopic evaluation was performed after the animals were sacrificed.

STATISTICAL ANALYSIS

Statistical analysis was performed using SPSS 20.0 (IBM Corp., Armonk, NY, USA). For all quantitative measurements results were expressed as mean±standard deviation. The homogeneity of variances was tested with the Levene's test. Based on the small number of observations, a test of normality will have very poor power. As no obvious outlying values were observed, normally distributed data were assumed and groups were compared using the univariate analysis of variance. In case of significant differences, Bonferroni or Dunnett's T3 *post hoc* tests were performed. For evaluation of the angular deflection, differences between the individual areas and differences between systole and diastole were identified with the Student's t-test. With regard to the small sample size, p-values were cited with an exploratory intention only. The probability of a type I error was set to 5% (α=0.05).

Results

In eleven of twelve cases a cardiac CT was successfully performed and the mitral valved stent was evaluated. One animal died during the CT evaluation from an anaesthesia incident and was not available for evaluation (110° prototype).

STENT POSITION

CT evaluation confirmed correct stent position within the native mitral annulus in all cases **(Figure 3)**. An LVOT obstruction was detected in two of eleven cases (45°: n=1; 90°: n=1) **(Table 1)**. No paravalvular leakages (PVL) were detected in the 110°-angled group after successful stent implantation[13]. In the other two groups, mild and trace PVL was detected in both groups[14].

STENT EXPANSION

Minor deformations of the stent body were detected in all three groups **(Table 1)**. Diameters were lower in the 45° and 90° prototype groups (p≤0.44). Deviations of the predefined inner stent diameter were in a similar range in these groups. The 45° and 90° prototypes were slightly "ovalised" (<3 mm deviation of minimal and maximal diameters). The 110° prototype showed a greater deviation of minimal and maximal diameters (>4 mm).

EFFECTIVE OPENING AREA

The effective opening area of the stent valve was ≥4 cm^2 in seven out of eleven cases (45°: n=4; 90°: n=2; 110°: n=1) and greater than 2 cm^2 in the remaining four cases (90°: n=2; 110°: n=2) **(Table 1)**. The effective opening was larger in the 45° prototype group compared to the 110° prototype group (p=0.02).

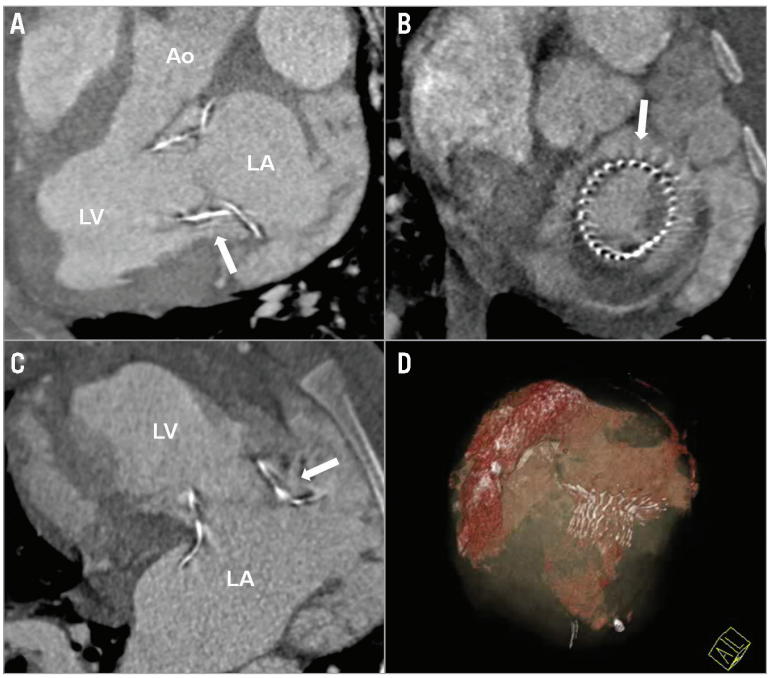

Figure 3. *A), B) & C) Cardiac CT short- and long-axis standard views showing correct stent position and no LVOT obstruction of the 110° prototype one month after implantation. Ao: aorta; LA: left atrium; LV: left ventricle (white arrow indicates the nitinol stent frame) D) Three-dimensional reconstruction showing the nitinol stent frame and left atrial and ventricular volumes.*

Table 1. LVOT obstruction evaluated in systole.

Animal	Design (atrio-ventricular j.)	Stent ID preset [mm]	Stent ID diastole		Stent ID systole		Effective opening area [cm²]	LVOT obstruction
			min [mm]	max [mm]	min [mm]	max [mm]		
1	45°	28.0	24.6	26.1	25.2	27.4	7.2	None
2		28.0	26.2	26.7	25.2	28.1	8.1	21%
3		28.0	24.2	26.8	24.5	25.3	7.4	None
4		28.0	24.0	25.6	22.2	26.1	8.0	None
Mean		28±0‡	24.7±1.0‡	26.3±0.6‡	24.3±1.4‡	26.7±1.3‡	7.7±0.4‡	
Deformation ΔD		n.a.	3.3±1.0	1.7±0.6	3.7±1.4	1.3±1.3	n.a.	
5	90°	27.0	22.8	25.8	23.2	25.1	7.4	43%
6		27.0	26.0	26.7	24.9	27.4	8.1	None
7¶		28.0	26.8	28.0	25.2	28.1	2.46	None
8		30.0	26.3	28.2	25.9	26.8	3.72	None
Mean		28±1.4‡	25.5±1.8‡	27.2±1.1‡	24.8±1.1‡	26.8±1.3‡	5.4±2.8	
Deformation ΔD		n.a.	2.5±1.7	0.8±0.8	3.2±0.9	1.2±1.7	n.a.	
9	110°	32.0	*	*	*	*	*	*
10		30.0	29.6	35.1	29.9	36.3	4.19	None
11		32.0	28.5	32.7	28.6	33.3	3.88	None
12		32.0	30.3	33.0	28.4	32.4	2.49	None
Mean		31.5±1.0	29.5±0.9	33.6±1.3	29.0±0.8	34.0±2.0	3.5±0.9	
Deformation ΔD		n.a.	1.9±1.6	–2.3±2.4	2.4±2.0	–2.7±3.2	n.a.	

Diastole evaluated at 65% ECG, systole evaluated at 20% ECG. Design: preset angle (45°, 90° or 110°) of the atrioventricular junction between ventricular stent body and atrial element; ID: inner diameter of the ventricular stent body; min: minimal diameter; max: maximal diameter; ΔD: maximal deformation of the preset diameter (ID_{preset} –$ID_{measured}$). *not to be evaluated (animal died of an anaesthesia incident); ¶animal with endocarditis; ‡p≤0.05 compared to the 110° prototype group

ANGULAR DEFLECTION

At the atrioventricular junction, large deformations of the stent structure were observed in all cases. The degree of deflection varied greatly in the four determined areas. Stents with a 45° and 90° angle exhibited a greater deflection of the preset stent geometry compared to stents with a 110° angle in all areas during systole and diastole (p≤0.032; **Table 2**). The greatest deflection of the 45° angled group was revealed in the anteromedial area (56.4°±14.5°, p≤0.18; **Figure 4**). The 110° stents displayed differences between the posteromedial area, and the posterolateral and anteromedial areas only in systole (p≤0.045). Deflection from the preset geometry was higher during diastole in all groups (p≤0.046).

TISSUE DIMENSIONS AND VOLUMETRIC ANALYSIS

Evaluation of left heart dimensions and volumetric analysis showed variable results **(Table 3)**. Hence, the significance of a comparison among the groups is depleted due to the limited number of animals. A tendency to smaller left atrial diameters was observed in the wide-angled 110° prototype group. Left ventricular volumetric analysis showed a tendency towards a higher ejection fraction in the group of wide-angled 110° prototypes. The end-diastolic volume was larger in the 90° and 110° prototype group compared to the 45° group (p≤0.048).

MACROSCOPIC EVALUATION

The macroscopic evaluation confirmed correct stent position within the native mitral annulus in all cases. In one of the four animals with a reduced effective mitral opening area, minor signs of endocarditis were detected; in the remaining three cases the leaflets were partly stiffened. Fractures of the nitinol stent frame were found more frequently in the 45° prototype group and occurred mainly in the area of the atrioventricular junction.

Table 2. Angular deflection (°) at the junction between atrial element and ventricular body.

		Anteromedial (septal)	Anterolateral	Posterolateral	Posteromedial
Narrow (45°)	20%	51.3±19.0*¶	37.1±25.4*¶‡	33.2±18.0*¶‡	25.5±14.2*¶‡
	65%	56.4±14.5¶	41.4±19.4¶‡	38.8±13.5¶‡	32.0±12.0¶‡
Medium (90°)	20%	17.8±1.6*¶	13.5±4.2¶‡	17.6±3.6*¶	14.5±5.1*¶
	65%	21.9±3.8¶	13.4±8.9¶	22.5±6.5¶	18.8±4.7¶
Wide (110°)	20%	16.4±5.4¶	17.6±5.0¶	17.1±1.3¶	12.1±3.4*¶‡
	65%	17.9±4.4¶	19.3±5.1¶	18.1±3.2¶	18.4±5.4¶

*$p \leq 0.05$ during comparison of the angular deflection during systole (20% ECG) and diastole (65% ECG) in this area, the angular deflection being defined as deviation of the angle α between ventricular and atrial element *in vivo* and the preset angle α (45°, 90°, 110°); ¶$p \leq 0.05$ compared to the 110° prototype; ‡$p \leq 0.05$ for evaluation of differences in comparison to the anteromedial area

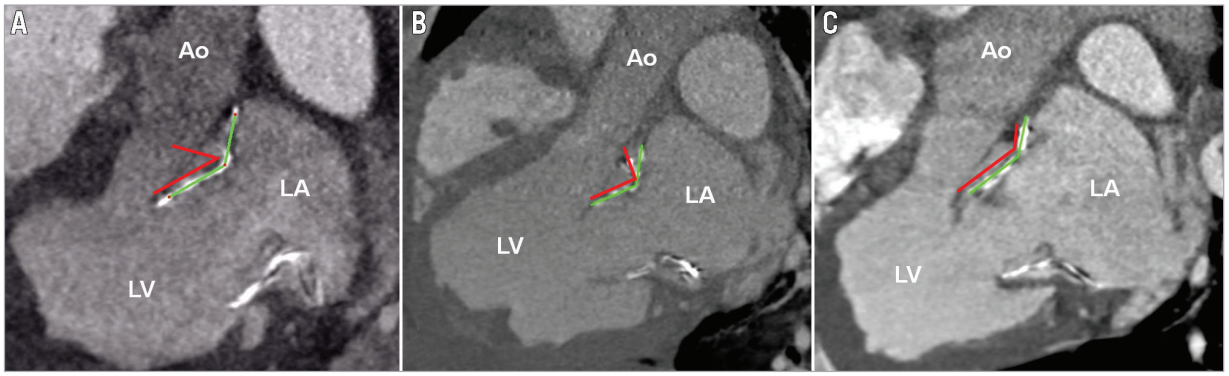

Figure 4. *Cardiac CT long-axis views showing the stent deflection in the anteromedial (septal) area. The red lines indicate the preset design, the green lines the in vivo stent shape. A) Prototype N (45°); B) Prototype M (90°); C) Prototype W (110°); Ao: Aorta; LA: left atrium; LV: left ventricle*

Discussion

The Euro Heart Survey revealed that surgery was denied to 49% of patients with severe symptomatic mitral regurgitation (MR) due to an impaired left ventricular ejection fraction, older age and comorbidities[16]. In future, the total number of patients suffering from MR will increase due to demographic changes[17], creating a rapidly growing demand for alternative, less invasive treatment options. An approach for treatment of MR to meet this requirement is the transapical implantation of a valved stent into the native mitral annulus in the beating heart[4-6]. Particular challenges for the development of such a device are the complex anatomy of the native mitral valve apparatus, the relative motion of the native mitral annulus and its position in the high-pressure system of the left heart. Previously, different studies have been published focusing on echocardiographic evaluation after mitral valved stent implantation in the beating heart[4,5,13,14]. In this study, the mechanical *in vivo* deformations of mitral valved stents have been quantified by computed tomographic analysis for the first time.

Cardiac CT is commonly used to analyse the native mitral valve and its pathological changes[18,19] and can provide valuable data during the development process. High-resolution, three-dimensional data acquisition and high reproducibility of adjusted views enable exact measurements, especially of experimental unusually-shaped devices. The study shows that design-related parameters can be quantified using CT and thus allow the identification of critical design areas.

STENT POSITION

Correct position was reproducibly shown, confirming the results of echocardiographic data[4]. An LVOT obstruction was observed in two out of eleven animals. This parameter is influenced by the patient's individual anatomy as well as the apical point of fixation and the relative stent size. Therefore, patient-specific planning will be of great importance in the clinical application of this new device.

STENT EXPANSION

An oval deformation of the valved stents was detected in all groups, indicating an adaptation to the oval shape of the native mitral annulus. This oval shaping may reduce the risk of paravalvular leakages

Table 3. Geometrical parameters and left volumetric analysis.

	Parameter	Narrow 45°	Medium 90°	Wide 110°	Native
LA dimensions	2-chamber view (mm)	63.2±3.2	51.1±9.8	52.8±5.0	45.3±8.6
	4-chamber view (mm)	50.3±8.3	46.5±5.0	42.3±5.8	49.1±5.3
	Height (mm)	27.7±6.9¶	37.1±2.7	40.9±3.3‡	25.6±5.4¶
	Circumference (cm)	19.5±9.3	19.3±2.3	20.7±2.9	15.9±1.0
LV dimensions	MV to apex (mm)	51.7±4.6‡	62.2±5.8¶	53.4±3.5	65.3±0.3¶
	MV to papillary muscle (mm)	20.0±5.7	20.1±1.3	17.4±0.3	16.5±1.1
	Septal thickness (mm)	10.4±2.1	9.4±1.5	8.3±2.9	8.1±0.3
	Myocardial thickness (mm)	10.3±2.6	12.2±2.9	9.5±2.4	6.2±1.8
LV volumetric analysis	EDV (cm^3)	81±8‡	114±41¶	117±15¶	108±28
	ESV (cm^3)	48±14	58±22	56±3	50±5
	EF (%)	40±17	49±11	51±8	53±7

LA dimensions evaluated at maximal atrial filling (40% ECG phase) and measured at 5 mm distance from valvular plane. LV, septum and myocardium dimensions evaluated at end diastole (80% ECG phase) in mid ventricular height. EDV: end-diastolic volume; EF: ejection fraction; ESV: end-systolic volume; *not to be evaluated (animal died of an anaesthesia incident); °not to be evaluated due to missing contrast; ¶$p \leq 0.05$ compared to the result marked with ‡

by improved alignment with the native structures. However, it implies the risk of central MR. It was noted that the oval deformation was greatest in the third group of 110° wide-angled stents. Due to its decreased thickness, the stent frame was less rigid and we suppose that it hence adapted more easily to the native geometry of the mitral annulus.

EFFECTIVE OPENING AREA

The effective opening area of the stent valves was normal (≥4 cm^2) in seven out of eleven cases. Endocarditic adhesions were found in one animal with reduced opening area. In the remaining three cases, mobility of the stent valve leaflets was partly reduced. Leaflet stiffening and defects caused by intrinsic calcification lead to mechanical failure of bioprosthetic heart valves[20]. One of the most important factors for the calcific failure is glutaraldehyde crosslinking[21]. Even though stenotic changes of the stent valve could have influenced the results of the study, these changes are not directly linked to the stent design. At the early experimental stage of this study, the development of an adequate stent design is the main challenge.

ANGULAR DEFLECTION

The deflection angle between the ventricular stent body and the atrial element proved to be a critical design parameter, allowing the quantification of the *in vivo* deformation of the atrioventricular junction. Hence, it directly relates to the mechanical stresses and is of the greatest importance for enhancement of long-term durability. Reduced *in vivo* deformation implies less stress in the nitinol frame and increased durability. However, we believe a certain deformation to be necessary to enable a secure stent position and good paravalvular sealing. Even though the number of animals in this study was relatively low, distinct tendencies were identified. The 45° narrow-angled prototype showed the greatest deformation, with deflection of up to 56°. The prototype design with a wide angle of 110° showed the least deflection of the preset angle providing optimal low deflection and good stability of the valved stents, reflected in good paravalvular sealing and the excellent wellbeing of the animals after an observation period of one month. Echocardiographic analysis after implantation of the wide-angled prototype showed no PVL directly after implantation and good health of the animals until planned euthanasia[13].

TISSUE DIMENSIONS AND VOLUMETRIC ANALYSIS

In contrast to the stent design-related parameters, left atrial and left ventricular dimensions were variable. Due to the limited number of animals, a comparison between the groups has limited validity. The smallest left atrial diameters after valved stent implantation were detected in the 110° wide-angled group. This correlates well with the general wellbeing of the animals, which was excellent after three weeks in this last group.

The volumes determined during the left ventricular volumetric analysis were within normal ranges for animals with a 90° and 110° prototype with a mean ejection fraction of 51.3% (110° group), being comparable to the baseline reference.

In addition to the important information to be derived from cardiac CT during the experimental development process of mitral valved stents, we believe it to be an important technique for the clinical use of such a device. It may prove to be an important tool during preoperative and postoperative planning and evaluation of a clinical mitral valved stent implantation, as commonly seen during TAVI procedures[11,12].

Limitations

In this study, the mitral valved stents were implanted into the hearts of healthy pigs with normal valves and physiological haemodynamics. The effectiveness of the valved stents in eliminating mitral regurgitation in pathological hearts has to be proven, and the effect of possible remodelling has to be analysed in future studies. The number of animals analysed in the different study groups was low due to the early experimental stage of this study.

Conclusion

Good *in vivo* performance of the mitral valved stents was demonstrated at a high reproducibility. The results of the cardiac CT evaluation quantify the mechanical deformation of valved stents throughout the heart cycle, identifying critical areas within the stent design (atrioventricular junction, "ovalisation"). The results of the computed tomographic comparison indicate that a larger preset angle of 110° leads to less stent deflection, improved stent alignment within the native anatomy and hence reduces the mechanical load and the risk of stent fractures. This study shows the effectiveness of cardiac CT for quantification of the *in vivo* stent deformation, highlighting the potential of this technique during the development process of novel devices.

Impact on daily practice

Minimally invasive off-pump implantation of a valved stent into the mitral position could be of large benefit, in particular for multi-morbid patients, often being non-compliant for standard surgery. Three design iterations of a self-expanding valved stent were compared following successful implantation into the mitral valve using multislice cardiac computed tomography (CT) to identify the superior design. This study highlights the effectiveness of cardiac CT for early application during the stent development process. An approach is presented for the first time to quantify the *in vivo* mechanical deformations of mitral valved stents using cardiac CT, identifying critical design areas and potential for stent design improvement. Thus, a technique is presented to enhance the stent development process at an early experimental stage.

Acknowledgements

The authors would like to thank Gerard Morvan and Bernd Ludwig as well as Jessica Boldt, Florian Bönke, Katharina Huenges, Mathias Gegenwart and Lennard Bax for their assistance during this study.

Funding

This project on mitral valve replacement was supported by the German Research Foundation, Bonn, Germany (Grant LU 663/8-1) and the DZHK (German Centre for Cardiovascular Research).

Conflict of interest statement

The authors have no conflicts of interest to declare.

References

1. Piazza N, Asgar A, Ibrahim R, Bonan R. Transcatheter mitral and pulmonary valve therapy. *J Am Coll Cardiol.* 2009;53:1837-51.

2. Iung B, Baron G, Butchart EG, Delahaye F, Gohlke-Bärwolf C, Levang OW, Tornos P, Vanoverschelde JL, Vermeer F, Boersma E, Ravaud P, Vahanian A. A prospective survey of patients with valvular heart disease in Europe: the Euro Heart Survey on Valvular Heart Disease. *Eur Heart J.* 2003;24:1231-43.

3. Ma L, Tozzi P, Huber C.H, Taub S, Gerelle G, von Segesser LK. Double-crowned valved stents for off-pump mitral valve replacement. *Eur J Cardiothorac Surg.* 2005;28:194-99.

4. Iino K, Boldt J, Lozonschi L, Metzner A, Schoettler J, Petzina R, Cremer J, Lutter G. Off-pump transapical mitral valve replacement: evaluation after one month. *Eur J Cardiothorac Surg.* 2012;41:512-7.

5. Attmann T, Pokorny S, Lozonschi L, Metzner A, Marczynski-Bühlow M, Schoettler J, Cremer J, Lutter G. Mitral valved stent implantation: an overview. *Minim Invasive Ther Allied Technol.* 2011;20:78-84.

6. Banai S, Jolicoeur EM, Schwartz M, Garceau P, Biner S, Tanguay JF, Cartier R, Verheye S, White CJ, Edelman E. Tiara: a novel catheter-based mitral valve bioprosthesis: initial experiments and short-term pre-clinical results. *J Am Coll Cardiol.* 2012;60:1430-1.

7. Otterstad JE, Froeland G, St John Sutton M, Holme I. Accuracy and reproducibility of biplane two-dimensional echocardiographic measurements of left ventricular dimensions and function. *Eur Heart J.* 1997;18:507-13.

8. Andreini D, Pontone G, Mushtaq S, Pepi M, Bartorelli AL. Multidetector computed tomography coronary angiography for the assessment of coronary in-stent restenosis. *Am J Cardiol.* 2010;105:645-55.

9. Chenot F, Montant P, Goffinet C, Pasquet A, Vancraeynest D, Coche E, Vanoverschelde JL, Gerber B. Evaluation of anatomic valve opening and leaflet morphology in aortic valve bioprosthesis by using multidetector CT: comparison with transthoracic echocardiography. *Radiology.* 2010;255:377-85.

10. Buzzatti N, Maisano F, Latib A, Cioni M, Taramasso M, Mussardo M, Colombo A, Alfieri O. Computed tomography-based evaluation of aortic annulus, prosthesis size and impact on early residual aortic regurgitation after transcatheter aortic valve implantation. *Eur J Cardiothorac Surg.* 2013;43:43-51.

11. Jabbour A, Ismail T, Moat N, Gulati A, Roussin I, Alpendurada F, Park B, Okoroafor F, Asgar A, Barker S, Davies S, Prasad SK, Rubens M, Mohiaddin RH. Multimodality imaging in transcatheter aortic valve implantation and post-procedural aortic regurgitation: comparison among cardiovascular magnetic resonance, cardiac computed tomography, and echocardiography. *J Am Coll Cardiol.* 2011;58:2165-73.

12. Marwan M, Achenbach S, Ensminger SM, Pflederer T, Ropers D, Ludwig J, Weyand M, Daniel WG, Arnold M. CT predictors of post-procedural aortic regurgitation in patients referred for transcatheter aortic valve implantation: an analysis of 105 patients. *Int J Cardiovasc Imaging.* 2013;29:1191-8.

13. Pokorny S, Huenges K, Bähr T, Hansen JH, Fischer G, Gross J, Morlock M, Cremer J, Lutter G. Transapical mitral valved stent implantation: Enhanced survival and decreased paravalvular leakages. *Int J Cardiol.* 2014;175:418-24.

14. Pokorny S, Dai H, Bähr T, Huenges K, Marczynski-Bühlow M, Morlock MM, Cremer J, Lutter G. Transapical mitral valve stent implantation: comparison between circular and D-shaped design. *EuroIntervention.* 2014;10:372-80.

15. Filsoufi F, Carpentier A. Principles of reconstructive surgery in degenerative mitral valve disease. *Semin Thorac Cardiovasc Surg.* 2007;19:103-10.

16. Mirabel M, Iung B, Baron G, Messika-Zeitoun D, Détaint D, Vanoverschelde JL, Butchart EG, Ravaud P, Vahanian A. What are the characteristics of patients with severe, symptomatic, mitral regurgitation who are denied surgery? *Eur Heart J.* 2007;28:1358-65.

17. U. Nations. Department of Economic and Social Affairs, Population Division (2011). World Population Prospects: the 2010 Revision. CD-ROM Edition. http://www.alapop.org/2009/Docs/ProjectionsSeminar/FinalPresentations/Presentation_RioNov2011_Heilig.pdf

18. Beaudoin J, Thai WE, Wai B, Handschumacher MD, Levine RA, Truong QA. Assessment of mitral valve adaptation with gated cardiac computed tomography: validation with three-dimensional echocardiography and mechanistic insight to functional mitral regurgitation. *Circ Cardiovasc Imaging.* 2013;6:784-9.

19. Higgins J, Mayo J, Skarsgard P. Cardiac computed tomography facilitates operative planning in patients with mitral calcification. *Ann Thorac Surg.* 2013;95:e9-11.

20. Schoen FJ. Cardiac valves and valvular pathology: update on function, disease, repair, and replacement. *Cardiovasc Pathol.* 2005;14:189-94.

21. Connolly JM, Bakay MA, Alferiev IS, Gorman RC, Gorman JH 3rd, Kruth HS, Ashworth PE, Kutty JK, Schoen FJ, Bianco RW, Levy RJ. Triglycidyl amine crosslinking combined with ethanol inhibits bioprosthetic heart valve calcification. *Ann Thorac Surg.* 2011;92:858-65.